Dynamics of tidewater surge-type glaciers in northwest Svalbard

Damien MANSELL,* Adrian LUCKMAN, Tavi MURRAY

Department of Geography, College of Science, Swansea University, Swansea, UK
E-mail: d.t.mansell@exeter.ac.uk

ABSTRACT. The evolution of ice dynamics through surges of four tidewater-terminating glaciers in northwest Svalbard is investigated by remote sensing. A 20 year time series of glacier surface flow speeds and frontal positions is presented covering the recent surges of Monacobreen, Comfortlessbreen, Blomstrandbreen and Fjortende Julibreen. Surface flow speeds were derived using feature tracking between pairs of ERS SAR and ALOS PALSAR images, while frontal positions were taken from the same imagery, as well as more frequent but lower-spatial-resolution Envisat Wide Swath Mode images. During all four surges, increased ice flow caused the tidewater margin to advance while the calving flux was initially reduced to near zero due to compressive stresses limiting crevasse propagation. As ice speed decreased, the terminus continued to advance, until the glacier's speed had returned to its pre-surge flow rate. Only at this time did the terminus start to retreat and peak iceberg calving flux was established. We conclude that terminus advance closely tracks glacier speed-up, that there is little mass loss through calving during the most active phase of the surge, and that seasonal cycles of terminus positions diminish during the active surge phase.

1. INTRODUCTION

Surge-type glaciers undergo non-steady ice flow whereby decadal-long quiescent periods of low activity and marginal retreat are punctuated by short-lived periods of rapid flow, where velocities increase by a factor of 10–1000 times (Meier and Post, 1969; Murray and others, 2003a). During quiescence, the glacier flows at a rate slower than the balance velocity, and a large store of ice is built up in the reservoir zone. During the active phase of the surge, glacier flow increases to a rate faster than the balance velocity, the glacier surface becomes heavily crevassed and the down-glacier transfer of ice mass takes place (Meier and Post, 1969). The glacier terminus may advance by several kilometres and, where the front is tidewater-terminating, the iceberg calving flux may also be greatly increased (Murray and others, 2003a).

During the active phase of the surge, the increased ice flux to the tidewater ice cliff and the advance of the terminus into potentially deeper offshore water can increase the iceberg calving flux (Dowdeswell, 1989; Vieli and others, 2001). The tidewater terminus may advance by several kilometres as was exemplified by Bråsvellbreen, which advanced up to 20 km when it surged in 1936–38 (Schytt, 1969). When the increased ice flux of the surge is matched closely with the advance of the terminus such as in Perseibreen (Dowdeswell and Benham, 2003), iceberg calving may not be enhanced and little mass may be lost in this way. Despite the large population of Svalbard tidewater-terminating surge-type glaciers (Błaszczyk and others, 2009), and the limited understanding of this phenomenon, observations of tidewater surging glaciers remain scarce.

As well as understanding calving losses during surges, determining the quiescent period duration is crucial for forecasting sea-level rise contributions of densely populated surge-type glacier regions such as Svalbard, North America, Iceland and the Pamirs. Overall cycle lengths in the archipelago are not well known since only five glaciers have been observed to surge more than once (Dowdeswell and others, 1991).

By assessing the changes of four tidewater-terminating glaciers in northwest Svalbard surge phases, we investigate the ice dynamics, timing of surge initiation and termination and the general nature of Svalbard surges. Ice flux and retreat rates are combined to investigate the controls of ice-dynamic regimes on the calving rate and to better understand the complex relationship of evolving calving rates during a surge. Where glaciers have been observed to surge for the second time, we provide insight into the overall cycle lengths of these glaciers.

2. SVALBARD SURGE-TYPE GLACIERS

Svalbard contains one of the largest glaciated areas in the Arctic (Hagen and others, 1993; Dowdeswell and Hambrey, 2002), covering ~36 600 km^2. Calving of icebergs makes up a substantial part of mass loss from the archipelago's ice masses, estimated to be 4 ± 1 km^3 a^{-1}, which includes a 1 km^3 a^{-1} contribution from the general retreat of Svalbard glaciers over the past 80 years (Dowdeswell and Hagen, 2004). Calving takes place from two main types of ice mass in Svalbard: tidewater-terminating glaciers, generally flowing within steep-sided fjords; and larger ice caps and outlet glaciers, which terminate in long sections of vertical ice cliffs (Błaszczyk and others, 2009).

Svalbard calving glaciers can be further divided into surge-type and non-surge-type. Only ~1% of the global glacier population is thought to be of surge type (Jiskoot and others, 2000), yet estimates for Svalbard surge-type glaciers vary between 13% (Jiskoot and others, 1998) and 54–90% (Lefauconnier and Hagen, 1991). Within this wide range, Błaszczyk and others (2009) estimate that of all the Svalbard tidewater-terminating glaciers, ~43% could be surge-type.

The fact that surge-type glaciers occur in clusters around the world, such as in Svalbard, implies that their distribution is a result of local variables, including geology, climate and topography (Clarke and others, 1986). The typical duration

*Present address: Department of Geography, College of Life and Environmental Sciences, University of Exeter, Exeter, UK.

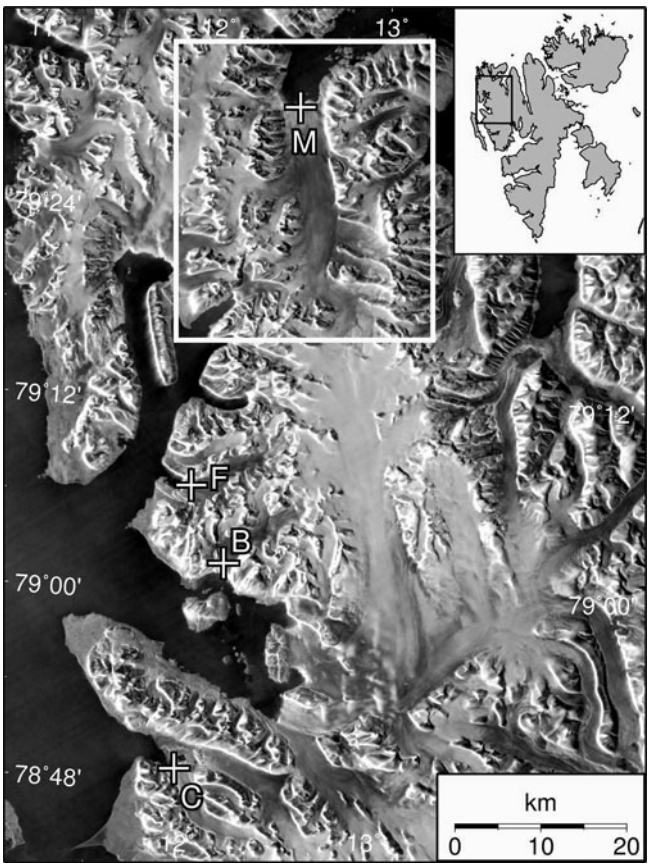

Fig. 1. Location of the four surge glaciers under investigation. The white crosses indicate the positions where the glacier flow speeds were extracted to produce the time series in Figure 3 for Monacobreen (M) (79°30′45″ N, 12°29′31″ E), Fjortende Julibreen (F) (79°06′44″ N, 11°58′39″ E), Comfortlessbreen (C) (78°48′52″ N, 11°57′44″ E) and Blomstrandbreen (B) (79°1′55″ N, 12°10′35″ E). The insert shows the location of the area within Svalbard. The white box shows the location of Figure 2. The underlying image is a 2009 annual average from Envisat Wide Swath Mode (WSM) scenes.

of the active phase of surge-type glaciers varies between these different clusters. Svalbard surge-type glaciers have a typical surge duration of 3–10 years. This is longer than for surge-type glaciers in North America, Iceland or the Pamirs, which typically have active surge phases lasting only 1–2 years (Dowdeswell and others, 1991). Svalbard glaciers also differ from Alaskan surging glaciers in that they do not exhibit such an abrupt termination of the active phase, which for Alaskan surges takes place in just a few days (Murray and others, 2003b).

The majority of Svalbard glaciers are polythermal (Hagen and Sætrang, 1991), meaning that parts of the ice masses are at the pressure-melting point (warm-based), while other parts remain at sub-freezing temperatures (cold-based). The presence of warm-based ice is a prerequisite for the active phase of glacier surges (Cuffey and Paterson, 2010). Svalbard surges are thought to be controlled by the thermal regime and to be initiated when cold parts of the bed are raised to the pressure-melting point and basal meltwater enhances sliding (Murray and others, 2000; Fowler and others, 2001).

Murray and others (2003b) noted that the nature of surge initiation and the presence of a surge front varies between tidewater and land-terminating glaciers. A surge front is a steep ramp of ice that separates fast-moving surging ice up-glacier, from slower-moving down-glacier ice (Murray and others, 1998). Surge fronts typically propagate downstream as a kinematic wave, often more rapidly than the ice itself (Raymond and others, 1987). Svalbard land-terminating glaciers such as Usherbreen and Bakaninbreen (Hagen, 1987; Murray and others, 1998) have exhibited clear surge fronts that initiated in the upper accumulation zone and propagated down-glacier. In contrast, observations of Svalbard tidewater-terminating glaciers such as Osbornebreen, Monacobreen, Perseibreen and Fridtjovbreen (Rolstad and others, 1997; Luckman and others, 2002; Dowdeswell and Benham, 2003; Murray and others, 2003a) provide evidence for surge initiation on the lower part of the glacier, without observed surge fronts. Despite these observations, Sund and others (2009) favor a theory of surge propagation down-glacier from the reservoir zone for both tidewater and land-terminating surge-type glaciers. These contradictions highlight the need for further tidewater-surge investigations.

3. STUDY AREA

This study focuses on surge-type glaciers in northwest Svalbard where valley tidewater-terminating glaciers are common. Figure 1 shows the location of the four surge-type tidewater-terminating glaciers investigated in this study: Monacobreen, Fjortende Julibreen, Comfortlessbreen and Blomstrandbreen.

Monacobreen (79°24′ N, 12°34′ E) is ~40 km long and flows north from Isachsenfonna ice cap into Liefdefjorden (Fig. 1). Based on satellite imagery and field reports from J.O. Hagen, the margin of Monacobreen retreated 0.75–1.45 km between 1966 and 1990 and then began to surge in the early 1990s (Luckman and others, 2002). Peak flow during the active-surge phase is thought to have occurred in January 1994, shown by the twofold increase of velocities from 1992 (Luckman and others, 2002; Strozzi and others, 2002). Radio-echo sounding (RES) was utilized by Bamber (1987) in the late 1980s to infer the glacial thermal regime. The RES showed an internal reflecton horizon (IRH) at ~120–200 m depth. The IRH obscures any bed return and suggests the glacier was warm-based over its accumulation area, thus providing further evidence of the glacier building to a surge initiation in the late 1980s to early 1990s.

Fjortende Julibreen, (79°07′ N, 12°13′ E) flows west from Isachsenfonna ice cap into Krossfjorden, is 16.2 km long and has a 1.84 km wide terminus (Błaszczyk and others, 2009). Interferometric synthetic aperture radar (InSAR) measurements from 1991 showed a maximum velocity close to the equilibrium line of ~0.07 m d^{-1} (Lefauconnier and others, 2001). Previous to this study, Fjortende Julibreen had not been observed to surge; however, as reported by Sexton and others (1992), Meier and Post (1969) note that Fjortende Julibreen may be a surge-type glacier in the quiescent phase.

Comfortlessbreen (78°46′ N, 12°88′ E) drains into Engelskbukta, south of the settlement of Ny-Ålesund. Only the southwest margin of Comfortlessbreen terminates in water. From 1990 to 2002, Comfortlessbreen retreated ~250 m (Sund and Eiken, 2010) and started to surge in 2006 (Sund and others 2009). Surface velocities from 2008 showed a 1 month average of ~2 m d^{-1} along the majority of the glacier length, which indicates block sliding, a characteristic of surging glaciers (Sund and Eiken, 2010).

Blomstrandbreen (79°1′ N, 12°10′ E) flows southwest into Kongsfjorden. This glacier surged around 1960 (Hagen and

others, 1993). During quiescence, Blomstrandbreen had retreated 2.5 km between 1966 and 2010 (Sund and Eiken, 2010), by which time it had completely withdrawn from the island Blomstrandhalvøya. From 2008 to 2009 the terminus of Blomstrandbreen showed a small advance, and compared with 1990 aerial photographs showed new and increased crevassing in 2007 and 2009 (Sund and Eiken, 2010). These are the first indications of a regime change from quiescence to an active surge phase since its last surge in the 1960s.

4. METHODS

4.1. Surface velocity

In this study we utilized synthetic aperture radar (SAR) data from the European Remote-sensing Satellite (ERS-1 and -2) missions from 1991 to 2010 archived by the European Space Agency (ESA), and from Fine Beam Single polarization (FBS) and Fine Beam Dual polarization (FBD) Advanced Land Observing Satellite (ALOS) Phased Array-type L-band SAR (PALSAR) from 2006 to 2010 archived by the Japan Aerospace Exploration Agency (JAXA). Over 70 image pairs were utilized per glacier. Glacier surface velocity was measured in both the slant-range and azimuth dimensions between repeat-pass satellite image pairs, by cross-correlating image patches in a process commonly referred to as feature tracking (Scambos and others, 1992; Strozzi and others, 2002). This technique has been widely used on tidewater outlet glaciers (e.g. Lucchitta and others, 1995; Luckman and others, 2003, 2006; Luckman and Murray, 2005), due to their heavily crevassed surface, which provides unique features that can be tracked between repeat images and has successfully measured glacier flow speeds on surging glaciers (e.g. Pritchard and others, 2005). Low-confidence correlations were discarded based on the strength of their signal-to-noise ratio, and also where the flow direction deviated significantly from the glacier flowline (Luckman and others 2006). The resulting glacier surface velocity maps allow comparisons across multiple satellite data types.

The velocity maps produced from feature tracking cannot be used to measure the strain rate (i.e. longitudinal stretching) arising from spatial variations in velocity. Because the strain rate requires a change in velocity, the feature-tracking errors are compounded and the uncertainties are beyond what is reasonable for the flow velocities of the glaciers in this study. Due to this measurement limitation, only point velocity measurements are used to investigate the evolution of flow speeds and calving rates through the surges. Errors from feature tracking arise from changes in the crevasse pattern through time and space, geometric transformations of the data, and errors in zero displacement reference points (Luckman and others 2006). The errors are estimated to be below $\pm 1\,\mathrm{m\,d^{-1}}$ and were calculated by measuring the displacements of features that are assumed to be stationary, such as rock-outcrops and nunataks (Pritchard and others 2005). For a given zero velocity reference point, the recorded displacement is therefore the error for that given image pair and surface velocity measurement. Multiple stationary features were selected, the apparent displacements of which were averaged for each image pair to calculate the error.

Due to the low velocities during quiescence and to the fact that Svalbard glaciers have low flow speeds in general, many of the quiescent flow speeds have large error estimates relative to the low flow-speed measurement. Although it is important to consider these error limits, the fact that there are multiple measurements which together show a strong underlying trend provides additional confidence for these values. This underlying trend is intrinsic to the glacier flow regime and is used to assess the timings of the surge. Flow speeds are presented with error bars determined directly from the errors estimated from zero references.

4.2. Frontal positions

Recent studies have measured terminus positions from satellite scenes to monitor seasonal and annual variations of the terminus of fast-flowing glaciers (e.g. Joughin and others, 2008a), tidewater-terminating glaciers (e.g. Vieli and others, 2002; Moon and Joughin, 2008; Ritchie and others, 2008), surging glaciers (e.g. Murray and others, 2003b; Jiskoot and Juhlin, 2009; Sund and Eiken, 2010) and ice shelves (e.g. Cook and others, 2005). The majority of these studies have used frontal positions digitized manually from geocoded satellite images. The Nyquist theorem determines the minimum sampling rate required to reasonably reconstruct a given signal. For an annual cycle that includes a seasonal fluctuation, at least four frontal positions per year are required (Ritchie and others, 2008). With investigations of multiple glaciers the process of manually digitizing fronts is very time-consuming and errors are dependent on the ability of the operator to effectively determine the boundary between the glacier front and the fjord.

In this study, tidewater-terminating fronts were measured using an approach that automatically detects the terminus position along a flowline on a georeferenced SAR scene. The calving front is detected from changes in the backscatter contrast between the bright, heavily crevassed terminus and the lower backscatter of the fjord. The border between high backscatter and significantly lower backscatter is the location of the terminus position along the flowline.

If the automatic detection technique does not recognize a significant contrast difference along the flowline, the terminus is unsuccessfully identified. This only occurs on rare occasions resulting from a change in backscatter of the fjord due to variable surface characteristics such as choppy surface waters or significant sea-ice cover. A visual inspection step is therefore carried out to check these outliers, as well as a general quality check on a portion of the scenes for each year. Where automatic detection of the terminus was rejected (<10%), manual digitization of the front was carried out.

Frontal positions were recorded from ERS SAR scenes throughout the time series and from November 2006 for the more frequent but lower-spatial-resolution Envisat Wide Swath Mode (WSM) data. More than 200 frontal positions were detected per glacier, with over 487 scenes for Monacobreen alone.

To measure the advance and retreat of the terminus, the position of the front was determined along transect lines measured from the position at the earliest image date. This study used the average frontal position from three parallel transect lines for each glacier, to account for non-uniform retreat across the ice front.

Both the manual digitizing and automatic detection procedures were tested for error by finding the position change of a rock outcrop border. The error is approximately equal to one pixel, which is ± 20 m for the ERS scenes and around ± 100 m for the Envisat WSM scenes. Although the

error for the Envisat WSM scenes is larger, the frontal positions recorded from the Envisat WSM data are consistent with those extracted from the ERS scenes.

4.3. Calving rate

The calving flux Q_c is defined as the volume of ice lost by iceberg calving from a tidewater-terminating glacier over any given time. It is usually measured in $m^3 d^{-1}$ and is calculated by:

$$Q_c = Q_{in} - \frac{V}{t}, \quad (1)$$

where the ice flux into the terminus from up-glacier is Q_{in}, the change in volume loss at the terminus is V, and t is the change in time (O'Neel and others, 2003). The calving flux calculation is not possible where the ice-cliff thickness is unknown, which along with water depth is the case for many Svalbard glaciers, including the glaciers in this study. For these glaciers the length calving rate can be used, which is a useful comparative measure of calving where ice thickness is not well known and is calculated by simplifying Equation (1). The length calving rate, U_c, is defined as the length of terminus discharged as icebergs per unit time ($m d^{-1}$). It is calculated from the terminus speed and change in the terminus position of tidewater-terminating glaciers,

$$U_c = U_T - \frac{L}{t}, \quad (2)$$

where U_T is the vertically average glacier flow speed and L is the change in terminus length. When L is negative there is a retreat; when L is positive, the terminus has advanced.

The length calving rate cannot be negative; however, on rare occasions the measured advance rate was greater than the measured speed U_T, as a result of lower measured velocity values than those at the terminus. On these occasions the length calving rate was set to zero to overcome this measurement issue. Annual length calving rates are required to compare changes in calving rates across the time series. In order to calculate the relevant annual averages for the velocity and frontal positions, seasonal values must be calculated. In order to avoid the annual averages being skewed by data-rich parts of the year compared to parts of the year with limited data coverage, seasonal values were calculated by taking the mean for a 3 month period. For example, a mean of the December–February values provided the winter average, and a mean of the June–August period provided the summer average. The annual frontal positions and flow speeds were then calculated by averaging the four seasonal values for that year. The resulting annual value is therefore unbiased across the year, despite different temporal coverage of the scenes, and variations in the coverage of robust flow speeds from feature tracking. Annual length calving rates were calculated by combining the annual frontal retreat/advance rates, and the speed at the terminus for each glacier.

5. ASSUMPTIONS AND LIMITATIONS

There are a number of assumptions made in calculating the length calving rate. The first is that the glacier speed used to calculate the length calving rate is approximately equal to that of the terminus. The flow speed close to the terminus is assumed to match that of the calving front due to the characteristic plug flow of surge-type glaciers (Schytt, 1969).

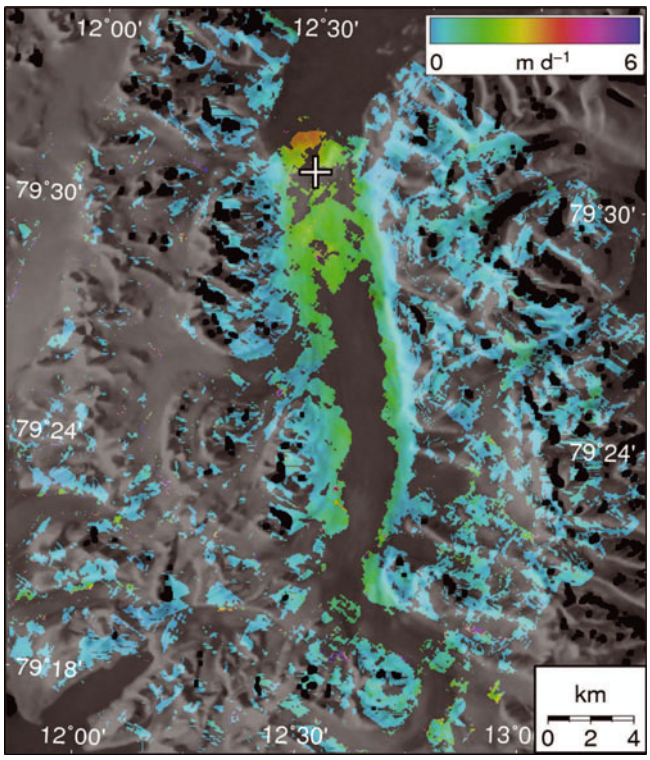

Fig. 2. Example velocity map during the surge of Monacobreen. Velocity values are indicated by the colour bar and are determined from feature tracking between ERS-1 image pairs from 19 October and 23 November 1995. The location of the image is shown in Figure 1.

Terminus flow speeds were not consistently available throughout the time series due to the increasingly chaotic nature of crevasses at the terminus, so robust flow speeds up-glacier from the chaotically crevassed zone were used which were approximately on the central flowline. The speed U_T, in Equation (2), was extracted from an area as close to the terminus as possible and produced robust flow-speed values for that location throughout the time series. The location of these points is shown in Figure 1 for each glacier. This enabled a much more robust and complete time series of glacier flow speeds which was used to calculate the length calving rate.

The length calving rate incorporates both calving and submarine melting at the terminus (Motyka and others, 2003). For the length calving rate to be applicable to the entire thickness of the glacier, it is assumed that the depth-averaged velocity, U_T, is equal to the surface flow speed, i.e. the glacier is sliding. This characteristic of sliding is typical of surging glaciers (Raymond, 1987). During times of quiescence, the glacier may or may not be sliding. In either case the error is small since U_T is $\geq$80% of the surface flow speed.

6. MEASURED ICE DYNAMICS AND CALVING RATES

To illustrate the coverage of velocity measurements, we present an example velocity map for Monacobreen from the peak of the surge (Fig. 2). Flow-speed measurement locations were chosen to be as close to the terminus as possible, and on the central flowline, with maximum available measurements throughout the time series, indicated by a white cross in Figure 1.

6.1. The active surge phase

Increased crevassing, terminus advance and increased glacier flow speeds indicated the active surge phase for each of the four tidewater glaciers in this study. For Monacobreen, surface flow rates increased to $4.5 \pm 0.6\,\mathrm{m\,d^{-1}}$ from $\sim 0.6\,\mathrm{m\,d^{-1}}$ during quiescence (Fig. 3a). The timings of changes in flow speed provide further evidence that the Monacobreen surge peaked between 1993 and 1995, which is in agreement with Strozzi and others (2002), who concluded the surge maximum was in 1994. The terminus advanced almost 2 km during the surge from its 1991 position, and the glacier continued to advance after velocities peaked. Annual calving rates show that although the surface flow speed had a nearly eightfold increase during the surge, the length calving rate showed no substantial variation for Monacobreen.

During the surge of Fjortende Julibreen, the glacier flow speed peaked in 2002, at a time when the terminus was advancing into the fjord. The calving rate is small for this glacier during quiescence and remains low during the surge (Fig. 3b). There is an observed decrease in calving rate during the surge, but this is within the error limits. The terminus continued to advance until the flow speed had returned to a pre-surge level, while maximum frontal advance occurred in 2004.

Comfortlessbreen demonstrated the same trend as Monacobreen and Fjortende Julibreen whereby the terminus continued to advance after the fastest flow phase. The maximum surface flow rate we measured during the Comfortlessbreen surge was in July 2008 when surface flow speeds were $1.95 \pm 0.25\,\mathrm{m\,d^{-1}}$ (Fig. 3c). This confirms previous measurements, which reported a July monthly average during 2008 of $2\,\mathrm{m\,d^{-1}}$ (Sund and Eiken, 2010). In 2004, before the surge had initiated, the terminus showed a small advance and small increase in flow speed. This small advance and subsequent retreat caused the annual mean length calving rate to increase in 2006. The length calving rate for Comfortlessbreen is small during both the quiescent period and the active surge phase, so care must be taken when interpreting changes within the error limits (Fig. 3c). During the active phase of the surge, the advance of the terminus was at a rate approximately equal to that of the increased ice flux to the terminus and so the length calving rate reduces from the 2006 annual mean.

The start of the active surge phase of Blomstrandbreen was captured at the end of 2007 when the flow speed increased and the terminus started to advance for the first time throughout the time series (Fig. 3d). By the beginning of 2009, the active surge phase was dominating the glacier dynamics and the flow speeds increased throughout the year. The increased flow speeds were accompanied by an advance of the terminus and the flow speeds continued to increase to the end of the time series in January 2010. Due to the shift from terminus retreat to terminus advance during the active surge phase, the annual length calving rate was at its lowest in 2008.

6.2. The quiescent surge phase and seasonal cycle

On all four glaciers, during quiescence a seasonal oscillation in the calving front was observed. During the summer the terminus retreat rates increased, whereas during the winter the retreat rates were restricted or in some years terminus advance took place. For the Comfortlessbreen surge the frontal positions showed seasonal variations of ~ 0.1 km, superimposed on a slow steady retreat from 1991 to 2004.

When the temporal sampling of glacier flow speeds was high, a seasonal pattern was observed in the glacier flow speeds. These observations are noisy due to uncertainty limits of the measurement technique and the low flow speeds of these glaciers. Maximum flow occurred in the summer, while flow speeds were reduced during the winter. This trend was most obvious when good temporal coverage of glacier flows speeds existed, and is shown in Figure 3 for Monacobreen during 2008–09 and for Blomstrandbreen from 2002 to 2006.

Monacobreen returned to quiescence at the end of 1997, when glacier flow speeds had reduced significantly and a steady retreat of the terminus was initiated. After 11 years of retreat, the terminus returned to the 1991 position, and a strong seasonal cycle in the calving front position was observed.

After the termination of the Fjortende Julibreen surge, the length calving rate increased and the glacier underwent a steady retreat. The rate of retreat decreased from 2008 onwards, along with the length calving rate, while the base speed remained steady at $\sim 0.2\,\mathrm{m\,d^{-1}}$ from 2005 to 2010. Although this value is below the error limits of the feature-tracking technique, it is an average over multiple years and describes the robust underlying trend for this time period.

Blomstrandbreen had a much larger retreat rate during quiescence compared to the other glaciers in this study. From 1991 to 2007, Blomstrandbreen retreated ~ 1.4 km. Superimposed on the overall retreat is the same seasonal cycle of reduced frontal retreat during the winter and enhanced retreat during the summer. This is particularly noticeable for 1991–2001 and 2002–07, when there is good temporal coverage for Blomstrandbreen (Fig. 3d).

7. DISCUSSION

7.1. Quiescent-phase dynamics

During the quiescent period prior to the surge, a seasonal cycle was evident in the terminus positions. This seasonal cycle was also observed after the surges of Monacobreen from 2007 onwards and Fjortende Julibreen from 2009 onwards. During these years, enhanced retreat occurred during the summer, while the rate of terminus retreat was reduced during the winter. The data show that annual fluctuations in front position are clearer than fluctuations in speed, suggesting that calving rate is the main driver of this pattern as opposed to changes in flow speeds driving calving. Possible drivers for the seasonal pattern of terminus advance/retreat could be due to meltwater availability and the influence of water in crevasses (Nick and others, 2010), or sea-ice buttressing during the winter, which is a significant factor for Greenland tidewater-terminating glaciers where ice melange is prevalent (Joughin and others, 2008b; Amundson and others, 2010).

Increasing summer velocities could be a driver for the seasonal fluctuations in terminus position due to increased extensional flow and crevassing. However, seasonal velocity variations cannot be confirmed for the glaciers in this study due to the limits of the data uncertainties. Seasonal velocity variations are observed for a nearby glacier, Kronebreen, which calves into Kongsfjord (Kääb and others, 2005). It is expected that this seasonal cycle is a common pattern for the quiescent glaciers in this study and other tidewater-terminating glaciers in northwest Svalbard. This seasonality

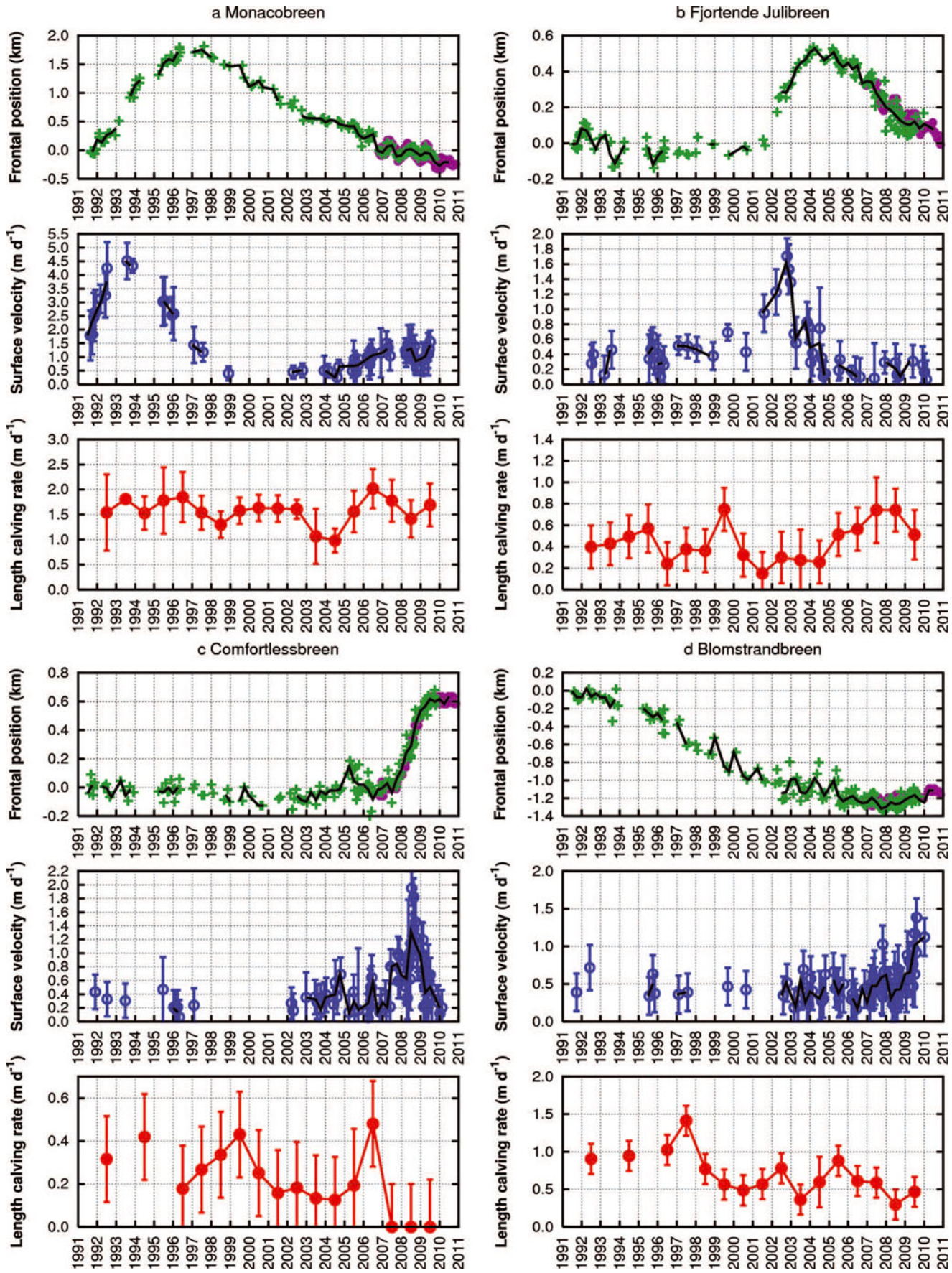

Fig. 3. Time series of measurements from 1991–2011 for (a) Monacobreen, (b) Fjortende Julibreen, (c) Comfortlessbreen and (d) Blomstrandbreen. The top panel for each glacier shows the frontal positions relative to the 1991 position where an advance is positive and retreat is negative. Frontal positions extracted from ERS scenes are plotted as green crosses; those from Envisat WSM scenes are purple circles. The black line is a plot of the seasonally averaged values to highlight seasonal variations. The middle panels show the surface flow speeds from feature tracking. The bottom panels show the length calving rates as annual means, in some cases using interpolated velocity measurements where feature-tracking measurements are not available.

is likely to be linked to the relationships between subglacial hydrology, meltwater availability and the drainage of surface and stored water to the bed (Lingle and Fatland, 2003).

A notable observation is that in the three glaciers that have already ceased to surge, the terminus continued to advance after maximum speeds had been observed. The larger flow regime and calving rate of Monacobreen is attributed to the larger drainage area of this glacier compared to the others in the study.

7.2. Active-surge-phase dynamics

During the active surge phase for the four glaciers observed in this study, the flow speed closely matched the rate of terminus advance, resulting in the calving rates remaining low, with no additional mass loss by iceberg calving. This was likely due to compressive stresses limiting transverse crevasse propagation and calving. A compressive flow regime at the terminus during the active phase suggests that the glacier front could be the surge front (Murray and others, 1998). If the surge front is at the terminus, this supports the notion that surges on tidewater-terminating glaciers initiate at the glacier front and most likely propagate up-glacier (Murray and others, 2003b).

On all four glaciers the seasonal variation in frontal positions was not observed during the active surge phase, as the dynamics of the surge dominated the flow regime and the glacier changed to a state of increased glacier flow and terminus advance. Late in the active phase as flow speeds started to decrease, the terminus continued to advance due to the above-average ice flux to the terminus. When flow speeds returned to magnitudes more common with those in quiescence, transverse crevasses which had opened up behind the terminus as a result of increased longitudinal strain rates and velocity gradients may have propagated to the terminus and encouraged calving by providing preferential lines of weakness (Benn and others, 2007). Increased crevassing may also explain the seasonal retreat pattern, whereby increased velocities during the summer and associated strain rates are likely to cause the crevasse density to increase, leading to enhanced calving during the summer and a reduced retreat rate or advance during the winter. In this mechanism, calving is controlled by the factors that control the ice thickness and velocity, with calving responding to the overall glacier dynamics, as opposed to calving events triggering dynamic changes up-glacier, such as flow acceleration (Benn and others, 2007).

7.3. Comparisons with other Svalbard surges

During the surge of Monacobreen, flow speeds increased nearly eightfold, whereas Fjortende Julibreen, Comfortlessbreen and Blomstrandbreen had an increase of approximately five times the base flow rate. This is lower than the 10–100-fold velocity increase that is typical of surging glaciers (Murray and others, 2003a). Monacobreen, Fjortende Julibreen and Comfortlessbreen all started to retreat once flow speeds had reverted to those associated with quiescence. Although only the initial retreat of Comfortlessbreen was captured in the time series, we expect the reduced ice flux to the terminus will remain low and the terminus is likely to undergo a long steady retreat.

During Blomstrandbreen's quiescent phase the terminus retreated 1.4 km from 1991 to 2007. This retreat rate is significantly greater than the retreat rates prior to the surge of the other glaciers in this study. For example, Monacobreen retreated 0.75–1.45 km between 1966 and 1990 (Luckman and others, 2002). The large retreat rates of Blomstrandbreen are likely to be explained by the fact that it retreated from a pinning point on the bed into deeper water away from the island Blomstrandhalvøya. Retreating into deeper water encourages fast flow and increased longitudinal strain at the terminus, promoting crevasse propagation and calving losses (Meier and Post, 1987).

The gradual onset and length of the active phase of the four surges in this study are in keeping with other surges in Svalbard (Meier and Post, 1969; Dowdeswell and others, 1991; Hodgkins and Dowdeswell, 1994; Murray and others, 2003b). Fjortende Julibreen had previously not been known to surge, but the measured flow-speed increase and terminus advance show a 3 year active phase for this glacier as well as for Comfortlessbreen, with a 7 year active phase for Monacobreen. Although the length of the active phase for Blomstrandbreen is yet to be determined since the surge is ongoing, the observed active surge phase from late 2007 through to 2010 is already longer than would be expected for North American, Icelandic or Pamir surges (Dowdeswell and others, 1991). This timing dissimilarity is due to the fact that Svalbard surges are slower, so the down-glacier transfer of mass from the reservoir zone takes place over longer time periods.

The large increases of glacier flow speed for Blomstrandbreen accompanied by glacier advance from the end of 2007 to 2010 show the first signs of a change of regime from quiescence to an active surge phase since the glacier last finished surging in 1966. This gives a surge cycle of $\sim$47 years for Blomstrandbreen, which is close to the lower limit for known Svalbard surges (Dowdeswell and others, 1991). Blomstrandbreen is one of only five glaciers that have been observed to surge twice (Dowdeswell and others, 1991). The surge cycles of these glaciers include 40 years for Tunabreen, 70 years for Hambergbreen, 110 years for Recherchebreen and 133 years for Fridtjovbreen (Dowdeswell and others, 1991; Hagen and others, 1993). Tunabreen has since surged in 2003–05, which is in keeping with a 40 year cycle and makes it the only Svalbard glacier known to have surged three times (personal communication from D. Benn, 2011).

Svalbard surge-type tidewater-terminating glaciers have been observed to increase in calving rate during the active surge phase (e.g. Etonbreen and Bråsvellbreen (Dowdeswell, 1989)). However, the calving rates for these observations were not well constrained but were inferred from observations of icebergs and the presence of brash ice at the terminus. During the surge a change in the type of iceberg calving typically occurs, from small bergs during quiescence to moderate-sized icebergs during the active surge phase (Dowdeswell, 1989). The observations of Monacobreen, Fjortende Julibreen, Comfortlessbreen and Blomstrandbreen support those from Persiebreen, which show terminus advance rates closely matching the increased flow rates of a surge (Dowdeswell and Benham, 2003). The glaciers in this study underwent terminus retreat after the point of maximum ice flux, highlighting the importance of the timings of the surge cycle when estimating short-term mass loss from iceberg calving.

8. CONCLUSIONS

From an analysis of ERS, ALOS and Envisat WSM SAR scenes the frontal positions, surface flow speeds and calving

rates of four tidewater-terminating surging glaciers in northwest Svalbard have been investigated. The gradual onset and length of the active phase of Monacobreen, Fjortende Julibreen, Comfortlessbreen and Blomstrandbreen are in keeping with other Svalbard surges. The initiation of the Blomstrandbreen surge at the end of 2007 shows the surge cycle length is ~47 years which is at the lower limit of known surge periods in Svalbard.

Despite the large increase in glacier flow, the calving rate did not increase during the active phase of each surge, as the terminus advance was at a rate similar to the increased flow. Terminus advance rates closely matched velocities during the active phase. After the maximum flow speed had been reached, the terminus continued to advance. We hypothesize that the terminus advance occurred when compressive stresses most likely limited crevasse propagation and calving. Calving rates increased only after the active phase of the surge had been completed, at which time the flow most likely returned to an extensional regime and calving took place along transverse crevasses at the terminus. This process supports the view of calving being driven by ice flux and terminus position changes, as opposed to the alternate view whereby calving triggers changes up-glacier, including flow acceleration (Meier and Post, 1987; Howat and others, 2005).

In all four glaciers a seasonal retreat pattern is observed during the quiescent period. Enhanced retreat occurred during the summer, while the rate of terminus retreat was reduced during the winter. During the active phase of each surge, the change in flow regime to a fast-flowing advancing glacier dominated the glacier dynamics, and the seasonal cycle was not observed at the scale of this study. Terminus retreat and an increase in calving was only observed after the active phase of the surge had completed. The results highlight the importance of understanding the timings and compressive/extensional flow regimes when quantifying calving losses of tidewater surge-type glaciers.

ACKNOWLEDGEMENTS

We are grateful to the European Space Agency for providing the ERS images (project C1P.7039, A03.103 and A03.283) and Envisat images (project GST/02/2192). We thank the Japan Aerospace Exploration Agency for providing the ALOS PALSAR scenes (project P100001). D. Mansell was funded by the UK Natural Environment Research Council (NE/F009062/1). We thank R.J. Motyka for review comments.

REFERENCES

Amundson JM, Fahnestock M, Truffer M, Brown J, Lüthi MP and Motyka RJ (2010) Ice mélange dynamics and implications for terminus stability, Jakobshavn Isbræ, Greenland. *J. Geophys. Res.,* **115**(F1), F01005 (doi: 10.1029/2009JF001405)

Bamber JL (1987) Radio echo sounding studies of Svalbard glaciers. PhD thesis, University of Cambridge.

Benn DI, Warren CW and Mottram RH (2007) Calving processes and the dynamics of calving glaciers. *Earth-Sci. Rev.,* **82**(3–4), 143–179.

Błaszczyk M, Jania JA and Hagen JO (2009) Tidewater glaciers of Svalbard: recent changes and estimates of calving fluxes**.** *Pol. Polar Res.,* **30**(2), 85–142

Clarke GKC, Schmok JP, Ommanney CSL and Collins SG (1986) Characteristics of surge-type glaciers. *J. Geophys. Res.,* **91**(B7), 7165–7180

Cook AJ, Fox AJ, Vaughan DG and Ferrigno JG (2005) Retreating glacier fronts on the Antarctic Peninsula over the past half-century. *Science,* **308**(5721), 541–544

Cuffey KM and Paterson WSB (2010) *The physics of glaciers*, 4th edition. Butterworth-Heinemann, Oxford

Dowdeswell JA (1989) On the nature of Svalbard icebergs. *J. Glaciol.,* **35**(120), 224–234

Dowdeswell JA and Benham TJ (2003) A surge of Perseibreen, Svalbard, examined using aerial photography and ASTER high-resolution satellite imagery. *Polar Res.,* **22**(2), 373–383

Dowdeswell JA and Hagen JO (2004) Arctic glaciers and ice caps. In Bamber JL and Payne AJ eds. *Mass balance of the cryosphere: observations and modelling of contemporary and future changes*. Cambridge University Press, Cambridge, 527–557

Dowdeswell JA and Hambrey MJ (2002) *Islands of the Arctic.* Cambridge University Press, Cambridge

Dowdeswell JA, Hamilton GS and Hagen JO (1991) The duration of the active phase on surge-type glaciers: contrasts between Svalbard and other regions. *J. Glaciol.,* **37**(127), 388–400

Fowler AC, Murray T and Ng FSL (2001) Thermally controlled glacier surging. *J. Glaciol.,* **47**(159), 527–538

Hagen JO (1987) Glacier surge at Usherbreen, Svalbard. *Polar Res.,* **5**(2), 239–252

Hagen JO and Sætrang A (1991) Radio-echo soundings of sub-polar glaciers with low-frequency radar. *Polar Res.,* **9**(1), 99–107

Hagen JO, Liestøl O, Roland E and Jørgensen T (1993) Glacier atlas of Svalbard and Jan Mayen. *Nor. Polarinst. Medd.* 129

Hodgkins R and Dowdeswell JA (1994) Tectonic processes in Svalbard tide-water glacier surges: evidence from structural glaciology. *J. Glaciol.,* **40**(136), 553–560

Howat IM, Joughin I, Tulaczyk S and Gogineni S (2005) Rapid retreat and acceleration of Helheim Glacier, east Greenland. *Geophys. Res. Lett.,* **32**(22), L22502 (doi: 10.1029/2005GL024737)

Jiskoot H and Juhlin DT (2009) Correspondence. Surge of a small East Greenland glacier, 2001–2007, suggests Svalbard-type surge mechanism. *J. Glaciol.,* **55**(191), 567–570

Jiskoot H, Boyle P and Murray T (1998) The incidence of glacier surging in Svalbard: evidence from multivariate statistics. *Comput. Geosci.,* **24**(4), 387–399

Jiskoot H, Murray T and Boyle P (2000) Controls on the distribution of surge-type glaciers in Svalbard. *J. Glaciol.,* **46**(154), 412–422

Joughin I and 8 others (2008a) Ice-front variation and tidewater behavior on Helheim and Kangerdlugssuaq Glaciers, Greenland. *J. Geophys. Res.,* **113**(F1), F01004 (doi: 10.1029/2007JF000837)

Joughin I and 7 others (2008b) Continued evolution of Jakobshavn Isbræ following its rapid speedup. *J. Geophys. Res.,* **113**(F4), F04006 (doi: 10.1029/2008JF001023)

Kääb A, Lefauconnier B and Melvold K (2005) Flow field of Kronebreen, Svalbard, using repeated Landsat 7 and ASTER data. *Ann. Glaciol.,* **42**, 7–13

Lefauconnier B and Hagen JO (1991) Surging and calving glaciers in eastern Svalbard. *Nor. Polarinst. Medd.* 116

Lefauconnier B, Massonnet D and Anker G (2001) Determination of ice flow velocity in Svalbard from ERS-1 interferometric observations. *Mem. Natl Inst. Polar Res.*, Special Issue 54, 279–290

Lingle CS and Fatland DR (2003) Does englacial water storage drive temperate glacier surges? *Ann. Glaciol.,* **36**, 14–20

Lucchitta BK, Rosanova CE and Mullins KF (1995) Velocities of Pine Island Glacier, West Antarctica, from ERS-1 SAR images. *Ann. Glaciol.,* **21**, 277–283

Luckman A and Murray T (2005) Seasonal variation in velocity before retreat of Jacobshavn Isbræ, Greenland. *Geophys. Res. Lett.,* **32**(8), L08501 (doi: 10.1029/2005GL022519)

Luckman A, Murray T and Strozzi T (2002) Surface flow evolution throughout a glacier surge measured by satellite radar interferometry. *Geophys. Res. Lett.,* **29**(23), 2095 (doi: 10.1029/2001GL014570)

Luckman A, Murray T, Jiskoot H, Pritchard H and Strozzi T (2003) ERS SAR feature-tracking measurement of outlet glacier velocities on a regional scale in East Greenland. *Ann. Glaciol.,* **36**, 129–134

Luckman A, Murray T, de Lange R and Hanna E (2006) Rapid and synchronous ice-dynamic changes in East Greenland. *Geophys. Res. Lett.,* **33**(3), L03503 (doi: 10.1029/2005GL025428)

Meier MF and Post A (1969) What are glacier surges? *Can. J. Earth Sci.,* **6**(4), 807–817

Meier MF and Post A (1987) Fast tidewater glaciers. *J. Geophys. Res.,* **92**(B9), 9051–9058

Moon T and Joughin I (2008) Changes in ice front position on Greenland's outlet glaciers from 1992 to 2007. *J. Geophys. Res.,* **113**(F2), F02022 (doi: 10.1029/2007JF000927)

Motyka RJ, Hunter L, Echelmeyer KA and Connor C (2003) Submarine melting at the terminus of a temperate tidewater glacier, LeConte Glacier, Alaska, USA. *Ann. Glaciol.,* **36**, 57–65

Murray T, Dowdeswell JA, Drewry DJ and Frearson I (1998) Geometric evolution and ice dynamics during a surge of Bakaninbreen, Svalbard. *J. Glaciol.,* **44**(147), 263–272

Murray T and 6 others (2000) Glacier surge propagation by thermal evolution at the bed. *J. Geophys. Res.*, **105**(B6), 13 491–13 507

Murray T, Luckman A, Strozzi T and Nuttall A-M (2003a) The initiation of glacier surging at Fridtjovbreen, Svalbard. *Ann. Glaciol.,* **36**, 110–116

Murray T, Strozzi T, Luckman A, Jiskoot H and Christakos P (2003b) Is there a single surge mechanism? Contrasts in dynamics between glacier surges in Svalbard and other regions. *J. Geophys. Res.,* **108**(B5), 2237 (doi: 10.1029/2002JB001906)

Nick FM, Van der Veen CJ, Vieli A and Benn DI (2010) A physically based calving model applied to marine outlet glaciers and implications for the glacier dynamics. *J. Glaciol.,* **56**(199), 781–794

O'Neel S, Echelmeyer KA and Motyka RJ (2003) Short-term variations in calving of a tidewater glacier: LeConte Glacier, Alaska, USA. *J. Glaciol.,* **49**(167), 587–598

Pritchard H, Murray T, Luckman A, Strozzi T and Barr S (2005) Glacier surge dynamics of Sortebræ, east Greenland, from synthetic aperture radar feature tracking. *J. Geophys. Res.,* **110**(F3), F03005 (doi: 10.1029/2004JF000233)

Raymond CF (1987) How do glaciers surge? A review. *J. Geophys. Res.,* **92**(B9), 9121–9134

Raymond C, Jóhannesson T, Pfeffer T and Sharp M (1987) Propagation of a glacier surge into stagnant ice. *J. Geophys. Res.,* **92**(B9), 9037–9049

Ritchie JC, Lingle CS, Motyka RJ and Truffer M (2008) Seasonal fluctuations in the advance of a tidewater glacier and potential causes: Hubbard Glacier, Alaska, USA. *J. Glaciol.,* **54**(186), 401–411

Rolstad C, Amlien J, Hagen JO and Lundén B (1997) Visible and near-infrared digital images for determination of ice velocities and surface elevation during a surge on Osbornebreen, a tidewater glacier in Svalbard. *Ann. Glaciol.,* **24**, 255–261

Scambos TA, Dutkiewicz MJ, Wilson JC and Bindschadler RA (1992) Application of image cross-correlation to the measurement of glacier velocity using satellite image data. *Remote Sens. Environ.,* **42**(3), 177–186

Schytt V (1969) Some comments on glacier surges in eastern Svalbard. *Can. J. Earth Sci.,* **6**(4), 867–873

Sexton DJ, Dowdeswell JA, Solheim A and Elverhøi A (1992) Seismic architecture and sedimentation in northwest Spitsbergen fjords. *Mar. Geol.,* **103**(1–3), 53–68

Strozzi T, Luckman A, Murray T, Wegmuller U and Werner CL (2002) Glacier motion estimation using satellite-radar offset-tracking procedures. *IEEE Trans. Geosci. Remote Sens.,* **40**(11), 2834–2391

Sund M and Eiken T (2010) Correspondence. Recent surges on Blomstrandbreen, Comfortlessbreen and Nathorstbreen, Svalbard. *J. Glaciol.,* **56**(195), 182–184

Sund M, Eiken T, Hagen JO and Kääb A (2009) Svalbard surge dynamics derived from geometric changes. *Ann. Glaciol.,* **50**(52), 50–60

Vieli A, Funk M and Blatter H (2001) Flow dynamics of tidewater glaciers: a numerical modelling approach. *J. Glaciol.,* **47**(159), 595–606

Vieli A, Jania J and Kolondra L (2002) The retreat of a tidewater glacier: observations and model calculations on Hansbreen, Spitsbergen. *J. Glaciol.,* **48**(163), 592–600

MS received 23 March 2011 and accepted in revised form 9 September 2011